CHAPTER 4

Variability in Indian summer monsoon strength in the northeast Himalaya during the last millennium with major emphasis on extreme events

Chapter 4: Variability in Indian summer monsoon strength in the northeast Himalaya during the last millennium with major emphasis on extreme events

4.1 Introduction:

Indian summer monsoon rainfall critically impacts the socio-economic and cultural development of one–third of world's population in south Asia, by influencing the regional hydrological conditions. The northward movement of the ITCZ during boreal summers pulls the warm, moist winds from the Indian Ocean towards the Asian landmass (Overpeck et al., 1996; Fleitmann et al., 2003; Gadgil, 2003). The abrupt strengthening and failure of the ISM led to floods and droughts in South Asia, causing decrease in food grain production that eventually put an overburden on Indian economy. For example, the intriguing drought of 2002 had large effect on the Indian economy by pulling down the Gross Domestic Product (GDP) of the country by almost 1% (Gadgil et al., 2003).

In last few decades, an increase in the intensity and frequency of wet and dry spells has been observed in the rainfall pattern of India (Allan and Soden, 2008; Singh et al., 2014). The modelling studies also suggest arise in the frequency of extreme precipitation events in future owing to increased land-ocean thermal contrast and the convective activities with increasing global temperatures (Allan and Soden, 2008; IPCC, 2013). This atmospheric warming may result into longer summers and shorter winters that will induce the longer rainfall season with earlier onset and later withdrawal of monsoonal winds (Kitoh et al., 2013; Singh et al., 2014). The higher altitudes will receive more precipitation as rain due to the rise in temperature and in turn strengthening of tropical monsoon systems and more moisture transport due to higher evaporation in the oceans (Pavelsky et al., 2012).

Several palaeoclimatic studies indicate large fluctuations in ISM rainfall intensity over the past millennium; strong monsoon during MWP and CWP as well as a weak ISM during the LIA (Thompson et al., 2000; Anderson et al., 2002, Sinha et al., 2011; Singh et al., 2015). The abrupt occurrence of multidecadal drought and intense flood events during these intervals triggered the collapse of several dynasties in the South Asian region such as Yuan and Ming dynasty in China (Zhang et al., 2008; Cook et al., 2010), Angkor Wat in Cambodia (Buckley et al., 2010; Day et al., 2012). But such kinds of studies are lacking from the Indian subcontinent due to scarcity of high resolution records of rainfall variability from the continental archives. Also the available records present an equivocal picture of ISM rainfall changes in different parts of the country. Speleothem studies from India record an antiphase correlation between monsoon rainfall in Central India and NE India (Sinha et al., 2011); the heavier precipitation was observed in NE India during the LIA. The oxygen isotope ratio in speleothems is known to be robust indicator of monsoonal strength in South Asia which capture the isotopic signature of meteoric precipitation (Dansgaard et al., 1964; Pausata et al., 2011; Sinha et al., 2011; Dutt et al., 2015). The meteoric precipitation in the region reflects the changes in isotopic composition of the source regime, moisture source, the fractionation at the source and process taking place along the transport pathway.

In the present study, the ISM rainfall variability in India during the last millennium has been investigated, with major emphasize on the occurrence of extreme rainfall events and their role in determining the face of the Indian History, using the stable isotopic investigations of speleothem WSS-3 from the Wah Shikar cave, Meghalaya, NE India. The better understanding of frequency and intensity of these extreme events in the past and their forcing mechanisms are also crucial for improving our climate models and predictive capabilities for future planning strategies. The Wah Shikar cave is suitable to track past changes in the ISM rainfall pattern because ~80% of the annual precipitation in the region is contributed by the ISM between June and September (Sarma, 2005; Murata et al., 2007; Sinha et al., 2011).

4.2 Results

4.2.1 $\delta^{18}O$ and $\delta^{13}C$ ratios in speleothem calcite

The $\delta^{18}O$ ratio varies from -7.0 to -4.3‰ (Figure 4.1). This large range in the $\delta^{18}O$ values indicates that the isotopic signatures are primarily derived from the precipitation and temperature has played a little or no role during speleothem formation. Around 11°C temperature range is required for the same fractionation in oxygen isotope during carbonate deposition (Dorale et al., 1998; Lachniet, 2009). In $\delta^{18}O$ time series of the Wah Shikar cave, three different phases are observed, (i) the highest fluctuations have been observed from AD 1,026 to 1,320. The values are generally low and two phases of much depleted values have been observed from AD 1,180 to 1,210 and AD 1,290 to 1,320. The values are very high between AD

1,140 and 1,170. (ii) From AD 1,320 to 1710, the $\delta^{18}O$ values are moderate with a secular trend. Three phases of high values have been observed from AD 1,320 to 1,370, 1,440 to 1,470 and AD 1,660 to 1,710, (iii) From AD 1,710 to the Present, the $\delta^{18}O$ values show a gradual decreasing trend. The decadal scale abrupt changes are more frequent in the latter interval (Figure 4.1).

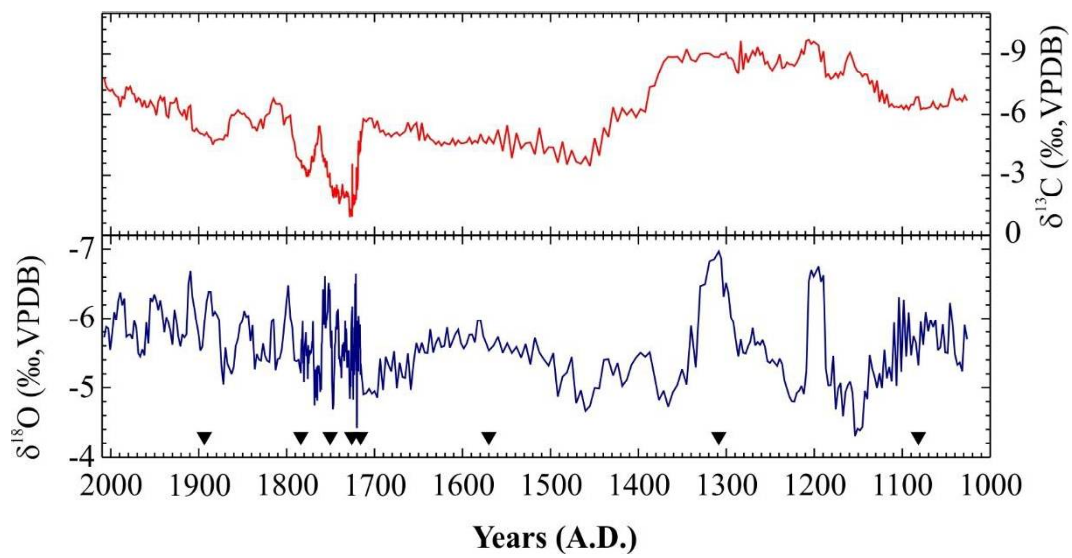

Figure 4.1 Indian summer monsoon proxy record of stable oxygen and carbon isotopes from Wah Shikar cave, Meghalaya, NE Himalaya for the period AD 1,026 to 2,012. The inverted black triangles in the bottom panel indicate the ^{230}Th ages

The $\delta^{13}C$ values vary from -9.7 to-0.9‰ (Figure 4.1). The values are low between AD 1,026 and 1,370. Around AD 1,370, the values abruptly increased and remained high until AD 1,800, except a brief phase of decreased values during AD 1,760 to 1,770. After AD 1,800, the values gradually decreased till the Present.

4.2.2 Hendy test

Hendy test is the correlation between $\delta^{18}O$ and $\delta^{13}C$ values of whole stalagmite sample or the subsamples of single lamina taken from central axis to margin (Hendy, 1971). This depicts the state of isotopic equilibrium or kinetic fractionation in the isotopic signature of speleothems during deposition (Hendy, 1971; Dreybrodt, 2008; Lachniet, 2009). The positive relationship between speleothem $\delta^{13}C$ and $\delta^{18}O$ values indicates that the isotopic signature of speleothem has been affected by the kinetic fractionation due to changes in cave temperature, ventilation or carbonate precipitation in soil horizon before the speleothem deposition etc. The correlation between 465 values of $\delta^{13}C$ and $\delta^{18}O$ from WSS-3 was determined which indicate no significant correlation (R^2= 0.02) between $\delta^{18}O$ and $\delta^{13}C$ ratios, hence the isotopic signatures are primarily reflect the isotopic equilibrium with the meteoric precipitation and hence the climatic signal (Hendy, 1971; Dreybrodt, 2008; Wiedner et al., 2008) (Figure 4.2). This assumption is further verified by the inverse relationship between our $\delta^{18}O$ record and 140 yrs June to September (JJAS) precipitation from NE India, showing a strong inverse relationship between rainfall and isotopic signatures of speleothem (Figure 4.3).

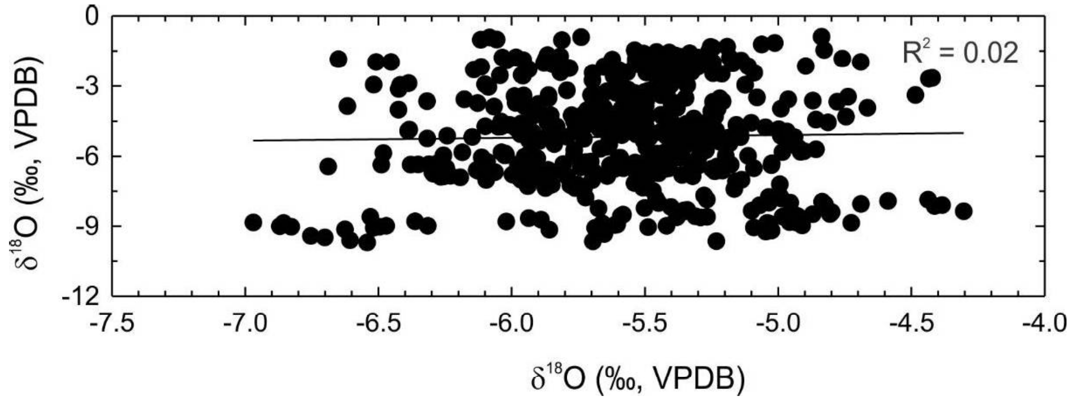

Figure 4.2 The Hendy test correlation between $\delta^{18}O$ and $\delta^{13}C$ proxy record from the Wah Shikar cave, NE Himalaya.

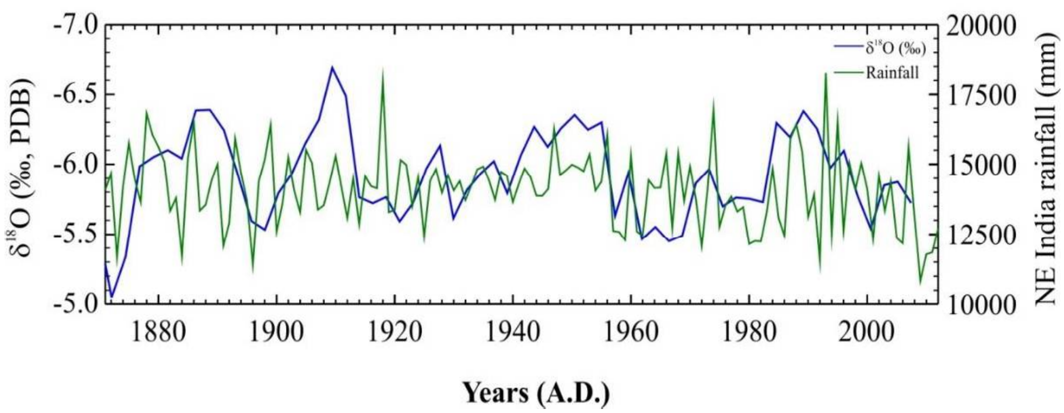

Figure 4.3 $\delta^{18}O$ proxy record from the Wah Shikar cave with the homogenous rainfall data in NE India from year 1871 to 2012 (http://www.tropmet.res.in/Data%20Archival-51-Page).

4.2.3 Spectral analysis

Spectral analysis of whole $\delta^{18}O$ time series indicates the periodicities of 21.3, 10.6, 8.40, 6.3 and 5.37 yrs during AD 1,026 to 2,007 (Figure 4.4). The spectral analysis of the record in three different segments as mentioned earlier indicates the cyclicity of 6.15 yrs between AD 1,026 and 1,320 (Figure 4.5); 14 and 8.37 yrs between AD 1,320 and 1,710 (Figure 4.6) and a strong cyclicity of 3.75 and 2.34 yrs from AD 1,710 to 2007 (Figure 4.7). The strong periodicities of 2-4 yrs are also observed in the instrumental rainfall data from NE India during AD 1,871 to 2,012 (Figure 4.8).

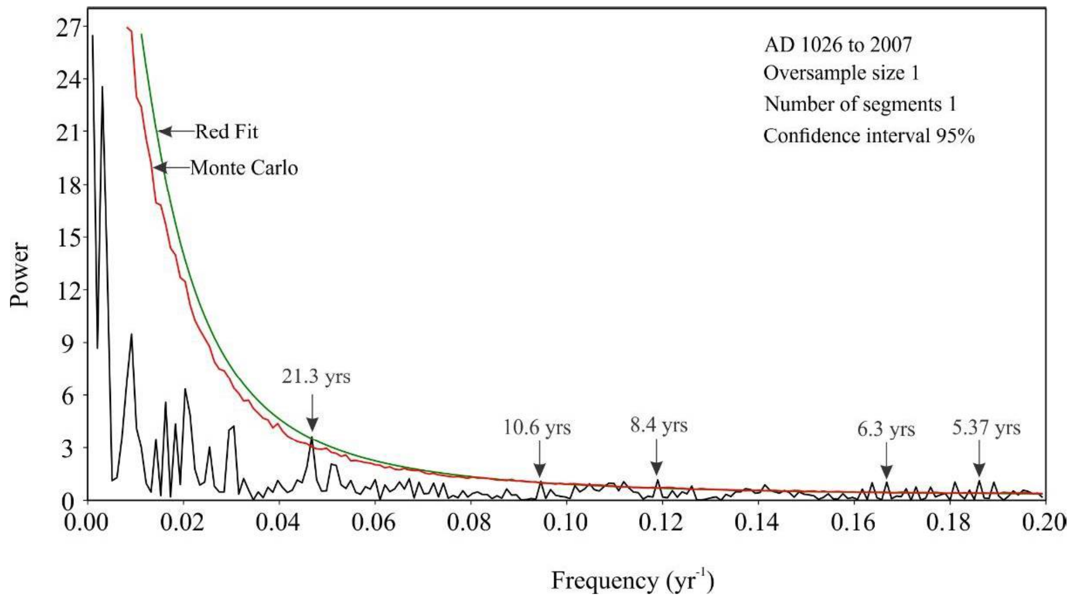

Figure 4.4 Spectral analysis of $\delta^{18}O$ time series from the Wah Shikar cave, Meghalaya, NE Himalaya from AD 1,026 to 2,007.

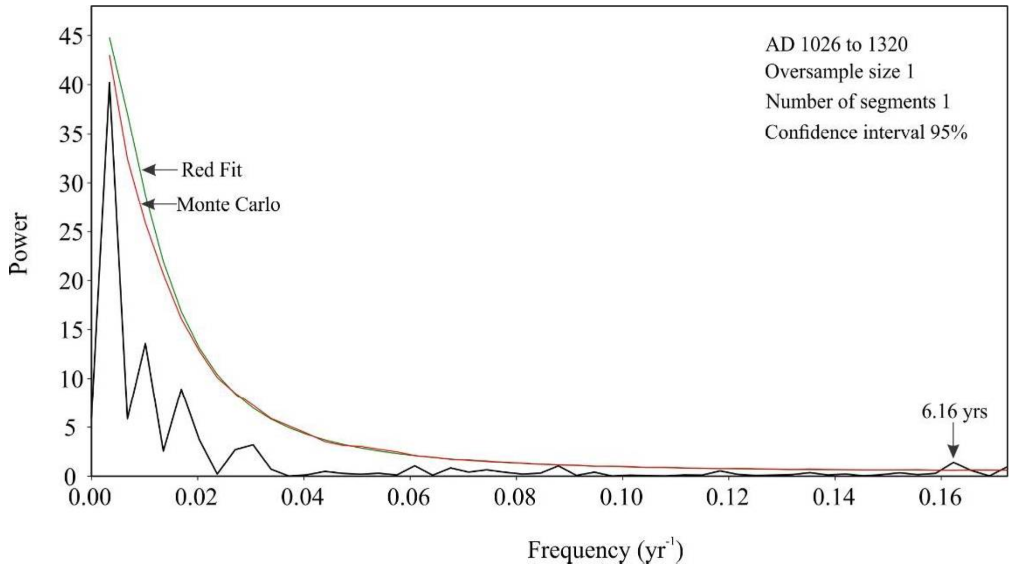

Figure 4.5 Spectral analysis of $\delta^{18}O$ time series from the Wah Shikar cave, Meghalaya, NE Himalaya from AD 1,026 to 1,320.

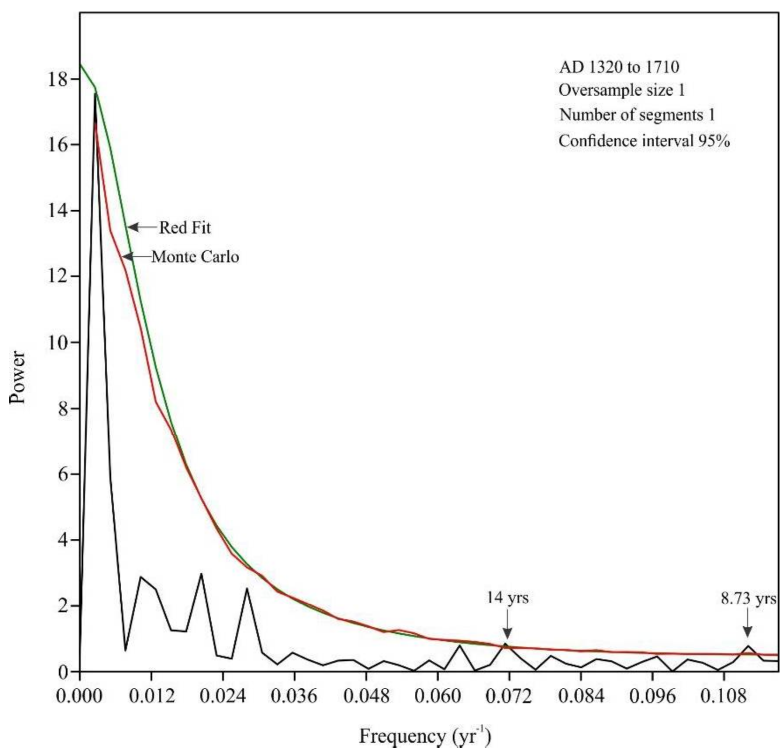

Figure 4.6 Spectral analysis of $\delta^{18}O$ time series from the Wah Shikar cave, Meghalaya, NE Himalaya from AD 1,320 to 1,710.

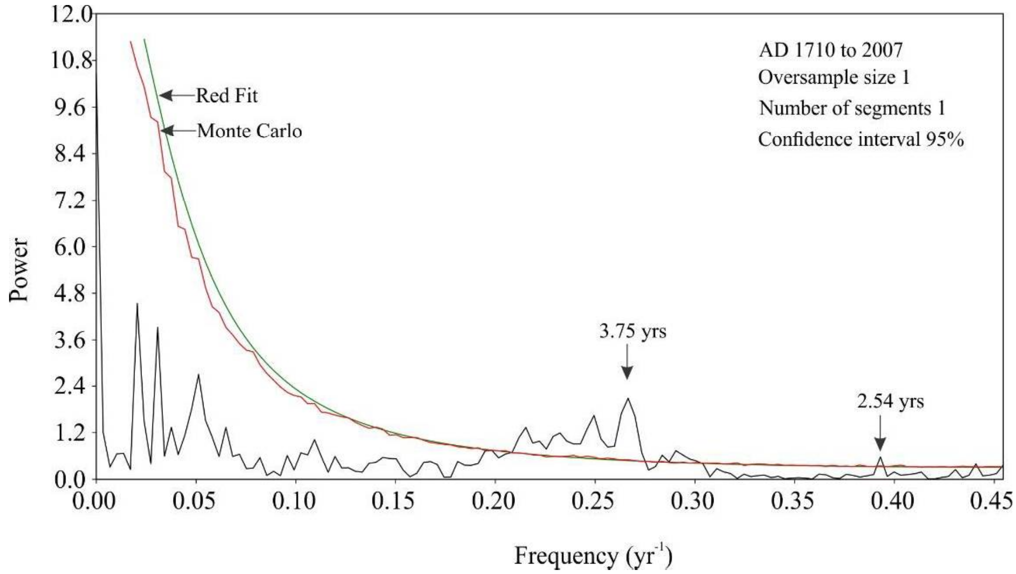

Figure 4.7 Spectral analysis of $\delta^{18}O$ time series from the Wah Shikar cave, Meghalaya, NE Himalaya from AD 1,710 to 2,007.

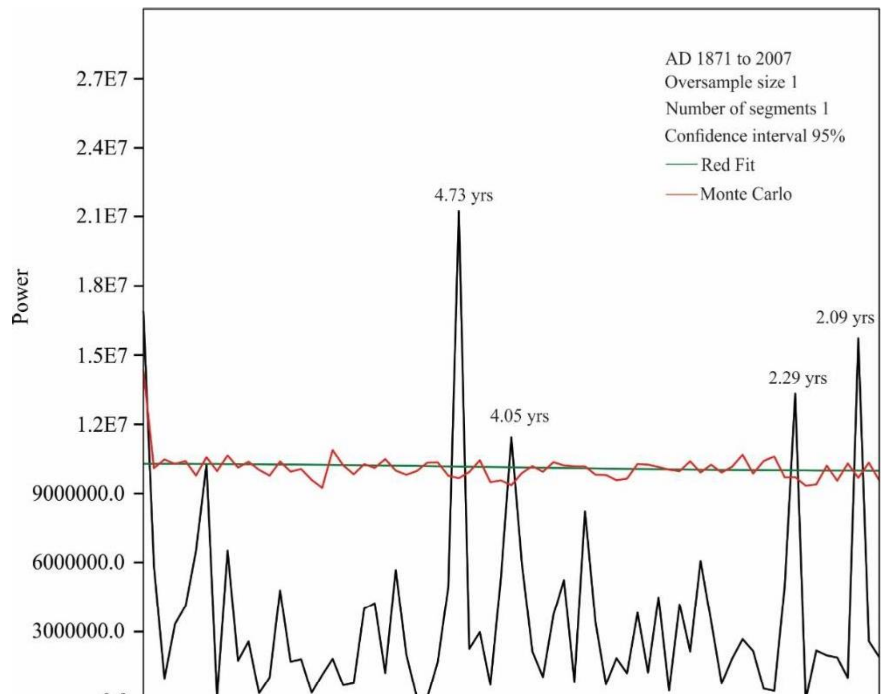

Figure 4.8 Spectral analysis of IITM homogenous rainfall data for NE India from years 1,871 to 2,012 (http://www.tropmet.res.in/Data%20Archival-51-Page).

4.3 Discussion

The large range of $\delta^{18}O$ values (-7 to -4.3‰) indicates that the rainfall intensity in the NE Himalaya was highly variable over the last 1000 yrs (Figure 4.1, 4.9). The trend of large scale fluctuations in the ISM strength, observed in this study is similar to that of palaeoclimatic records from Jhumar cave (Sinha et al., 2011), Dongge cave (Wang et al., 2005), Wanxiang cave (Zhang et al., 2008), and Arabian Sea (Anderson et al., 2002; Figure 4.9). This suggests that the behaviour of the ISM over the past millennium was similar throughout the South Asian region i.e. strong monsoon during the MWP and CWP and a weak monsoon during the LIA. Based on the $\delta^{18}O$ time series, variability of the ISM in the NE Himalaya during the last millennium can be categorised in three different phases:

(i) AD 1,026-1,320:

The low $\delta^{18}O$ values indicate a wetter climate during this interval (Figure 4.1, 4.9). This wetter climate can be attributed to strong ISM conditions during the MWP, also observed in several other palaeoclimatic records (Anderson et al., 2002; Gupta et al., 2003; Buckley et al., 2010; Sinha et al; 2011). The period ranging mid-12th century to the early 14th century recorded the highest fluctuations in rainfall intensity and witnessed prominent multidecadal drought and flood events, with two major floods events during AD 1200 and 1310.

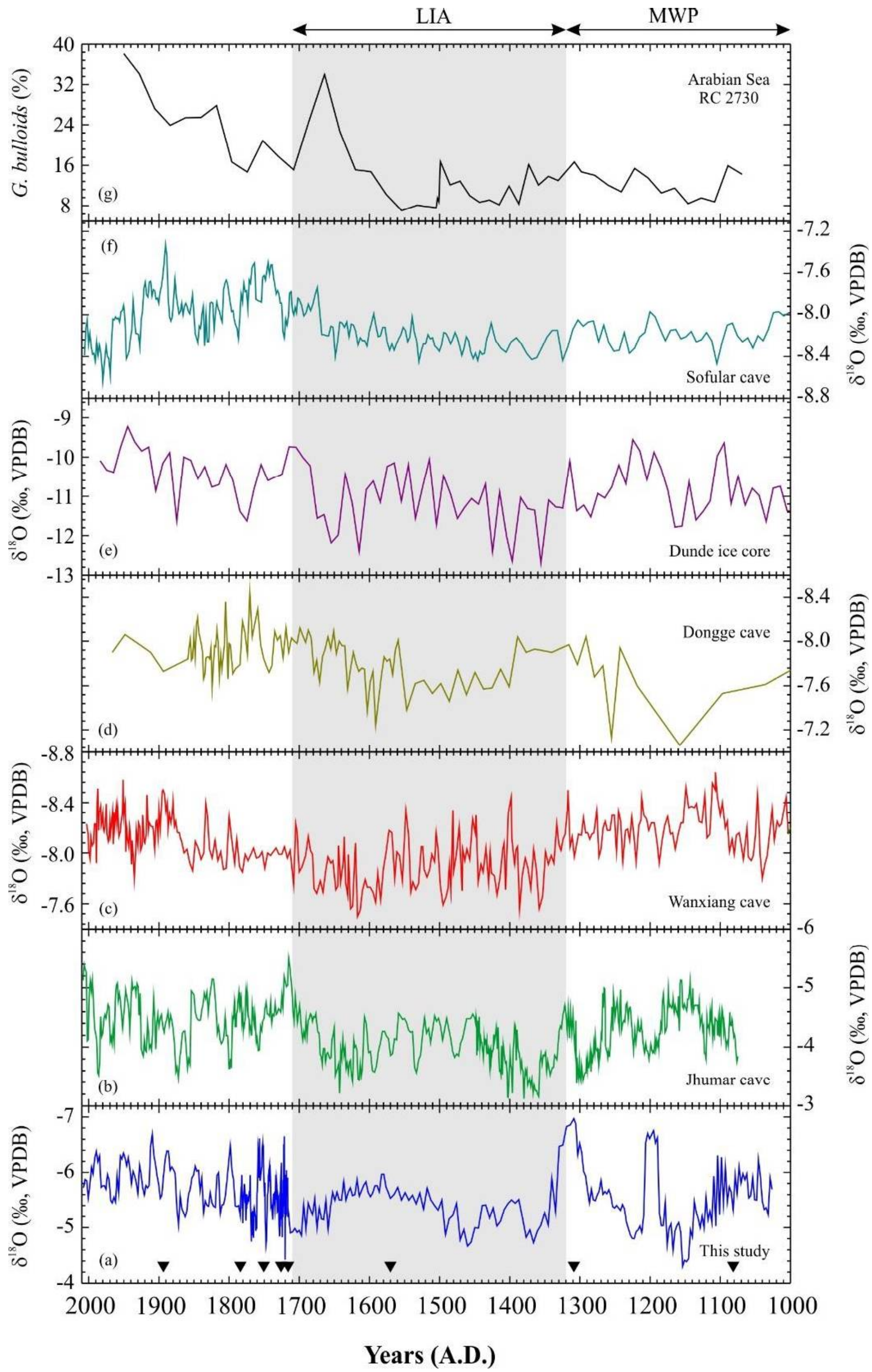

Figure 4.9 Indian simmer monsoon proxy record from Wah Shikar cave, Meghalaya, NE Himalaya compared with cave records from India, China and

Turkey; ice record from China and marine record from Arabian Sea. (a) $\delta^{18}O$ record from Wah Shikar cave, India (present study), (b) $\delta^{18}O$ record from Jhumar cave, India (Sinha et al., 2011), (c) $\delta^{18}O$ record from Wanxiang cave, China (Zhang et al., 2008), (d) $\delta^{18}O$ record from Dongge cave, China (Wang et al., 2005), (e) $\delta^{18}O$ record from Dunde ice core, China (Thompson et al., 2000), (f) $\delta^{18}O$ record from Sofular cave, Turkey (Fleitmann et al., 2009) and G. bulloides (%) in marine core RC 2730 from the Arabian Sea (Anderson et al., 2002). The inverted black triangles in the bottom panel indicate ^{230}Th ages. Light grey bar shows the Little Ice Age (LIA). The Medieval Warm Period (MWP) has also been shown.

(ii) AD 1,320-1,710:

The intensity of the ISM varied with a sudden weakening in the early 14th century (around AD 1,320) (Figure 4.1,4.9) because of atmospheric cooling during the LIA (Fleitmann et al., 2003; Gupta et al., 2003; Sinha et al., 2011). Although the onset and termination of the LIA were marked by prolonged drought phases, the abrupt climatic fluctuations were less during this time span. The cooling during this period caused the reduction in evaporation and convection in the Indian Ocean, and land-sea thermal contrast which resulted into low summer monsoon rainfall in Indian and adjoining regions (Anderson et al., 2002; Sinha et al., 2011; Singh et al., 2015).

(iii) AD 1,710 to the Present:

During the early 18th century (around AD 1,710), the intensity of the ISM started increasing with a rise in atmospheric temperature due to global warming coinciding with increased anthropogenic activities including the onset of the Industrial revolution in Europe. The ISM shows continuous strengthening till the Present (Figures 4.1, 4.9). Although the extremity of rainfall fluctuations in CWP is lesser than that occurred in the MWP, their frequency has increased considerably since the last three centuries (Figure 4.1, 4.9).

These changes in the climatic and rainfall patterns also largely determined the face of the Indian history (Cook et al., 2002; Sinha et al., 2011). Twelve major periods of feeble monsoon conditions in our record correlate well with the devastating famines occurred in India due to rainfall deficiency and caused loss of lives of millions of human and cattles (Table 4.1; Girdlestone, 1868; Williams, 1875; Dutt, 1901; Majumdar et al., 1978; Raychaudhuri et al., 1982; Kumar and Habib, 1983; Shewale and Kumar, 2005; Sinha et al., 2011). The establishment of Muslim rule and decline of several long-lasted dynasties in India from 12^{th} to 14^{th} century are contemporaneous with abrupt and extreme rainfall variability.

The prolonged droughts and heavy rainfall events during this period reduced the agriculture production and damaged the safety infrastructure; and made the Indian kingdoms weak and highly vulnerable to the local rebellions and external invasions that eventually captured most of the Indian subcontinent. The concurrent downfall of five powerful dynasties Kakatiya dynasty (1,323 AD), Paramara dynasty (1,327 AD), Seuna dynasty (1,334 AD), Hoysala dynasty (1,342 AD), Pandyan dynasty (1,345AD) in India (Table 4.2) can be linked with the sudden occurrence of multidecadal megadroughts after very high rainfall because of onset of the LIA that might have adversely affected the crop production (Majumdar et al., 1978; Raychaudhuri et al., 1982; Kumar and Habib, 1983).

The extensive Mughal Empire in India got disintegrated into several independent states during the late 17th and early 18th century due to multiyear droughts which followed the termination of the LIA (Majumdar et al., 1978; Raychaudhuri et al., 1982; Kumar and Habib, 1983). The poor crop productivity and trade raised the conflicts between these small states and helped in the eventual establishment of European rule in most of the South Asia region. Most of the wars that changed the direction of Indian political and cultural history were fought during the intervals of droughts and famines driven by the rainfall scarcity (Figure 4.10). The observed periodicity of 21.3, 14, 10.3 and 8.4 yrs in $\delta^{18}O$ time series in our record is the manifestation of solar insolation as a controlling factor to the ISM during the last millennium (Wang et al., 2005; Yadav and Ramesh, 2007). The periodicities of 4-6 yrs indicate the influence of ENSO circulation (Sikka, 1980; Gadgil, 2003). Similar cyclicity of ~4 yrs is also observed in the instrumental rainfall data from NE India. Bu Tree ring records from South Asia like Vietnam, Cambodia etc. (Sano et al., 2008, Buckley et al., 2010) also show a strong in-phase relationship between the multidecadal megadroughts and the strong El Niño events during the last millennium. But the relationship of the ENSO to the ISM is not constant throughout the time. The meteorological records of precipitation in India indicate the normal summer monsoon rainfall even in the presence of strong ENSO events, due to the influence of positive IOD (Ashok et al., 2001).

Table 4.1 List of major drought periods in Indian History.

Events No.	Drought Events	Drought years (A.D.)/ Major Famines
1.	2009-2002	2009 (-21.8) 2004 (-13.8) *2002 (-19.0)
2.	1982-1965	*1982 (-14.5) 1979 (-18.9) 1974 (-12.0) *1972 (-23.9) 1968 (-10.3) 1966 (-13.2) *1965 (-18.2)
3.	1920-1910	1920 (-16.7) *1918 (-24.9) 1913 (-10.0) *1911 (-14.7)
4.	1907-1899	1907 (-10.0) 1905 (-17.4) 1904 (-11.8) 1901 (-13.1) *1899 (-29.4)
5.	1878-1850	*1877 (-33.3) (1873-78) Bengal famine (1878) Famine in north India (1876-1878) Late Victorian drought
		(1868-70) Bengal famine (1865-70) Famine in Orissa and Rajputana
		(1860-61) Upper Doab famine (1853-55) Famine in Madras, Rajasthan and Bombay
6.	1840-1801	(1837-38) Famine in north west provinces (1832-33) Famine in Solapur and North Madras (1824-25) Deccan, Bombay and Madras famine (1820-22) Upper Sind famine (1819-20) North West Province, Rajasthan and Deccan (1812-13) Bombay, Kathiawar, Agra, Madras, Kucth (1803-04)Central India, Rajasthan and Karnatka
7.	1796-1760	(1790-1796) East India drought (1790-92) Bombay, Hyderabad, Gujarat, Kutch, North Madras and Orissa (1783) Bengal Famine (1770) Bengal famine (1752-1768) Strange parallel drought
8.	1715-1660	(1702-1704) Gujarat famine (1694-95) Delhi (1686-87) South India (1682-84) Deccan famine (1665) drought in NE India 1661 (Universal)
9.	1480-1450	(1452-1478) probable famine in Orissa
10.	1380-1334	(1361-62) North India (1345) All India (1334-41) North India (1330-1360)[10] Buckley et al., 2010
11.	1240-1210	Day et al., 2012
12.	1180-1140	(1148-1159)

* El Niño Year

Abrupt climatic changes are more frequent during warmer intervals than colder periods. Our record also indicates that during the last 1000 yrs, solar insolation and ENSO were the major forcing mechanisms for the ISM variability. The influence of ENSO was more in the warmer intervals while it weakened in colder intervals and solar insolation became a dominating driving mechanism (Rein, 2007). The ENSO prevented the northward migration of the ITCZ and caused several drought periods in the MWP and CWP. The incidences of extreme rainfall events in India have increased during CWP that may show further increase in near future with the rise in the global atmospheric temperature. The higher rainfall in the high altitude regions will increase the risk of flash floods and landslides in those areas along with the reduction in glacier extent that will affect India's water resources in decades to come.

Table 4.2 List of major dynasties in India which declined after 1000 A.D.

Sl No.	Dynasty	Time of Collapse	Time of rule
1.	Pala dynasty	1174 A.D.	750-1174 A.D.
2.	Tomar dynasty	1192 A.D.	736-1192 A.D.
3.	Chalukya dynasty of Kalyana	1200 A.D.	696-1200 A.D.
4.	Sena dynasty	1230 A.D.	1070-1230 A.D.
5.	Solanki dynasty	1243 A.D.	900-1243 A.D
6.	Cholas dynasty	1279 A.D	846-1279 A.D.
7.	Kakatiya dynasty	1323 A.D.	11th century-1323A.D.
8.	Paramara dynasty	1327 A.D.	800- 1327 A.D.
9.	Yadav dynasty	1334 A.D.	850-1334 A.D.
10.	Hoysala dynasty	1342 A.D.	1000-1342 A.D.
11.	Pandayan dynasty	1345 A.D.	6th century to 1345 A.D.
12.	Vijayanagar empire	1646 A.D.	1336-1646 A.D.
13.	Maratha Empire	1818 A.D.	1674-1818 A.D.
13.	Sikh empire	1849 A.D.	1799-1849 A.D.
14.	Mughal Empire	1857 A.D.	1556-1857 A.D.

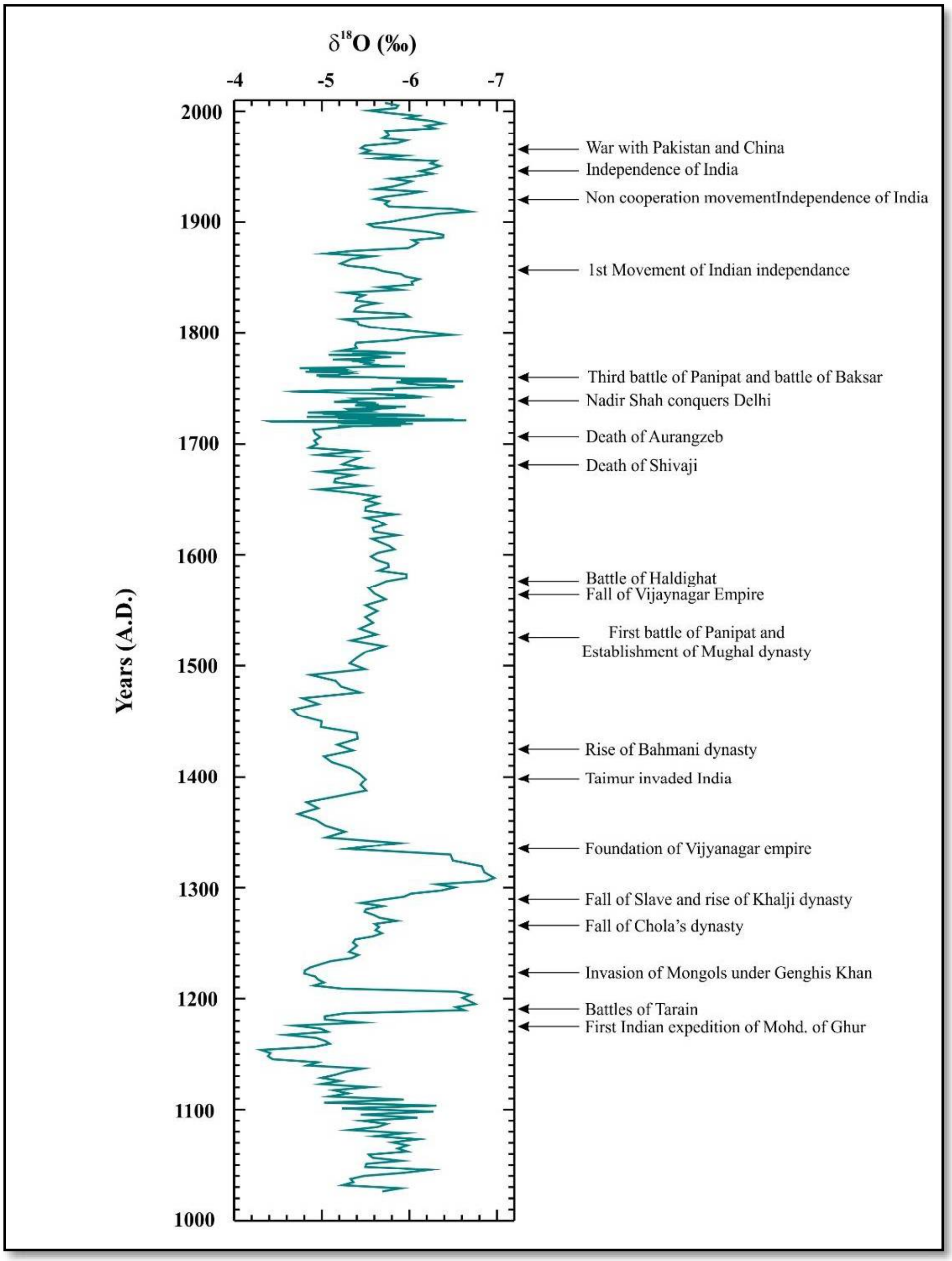

Figure 4.10 Correlation of Indian summer monsoon proxy record from the Wah Shikar cave with the major events in the Indian history during last the last millennium.